

# Planar Tri-Band Antenna Design

Michal POKORNÝ, Jiří HORÁK, Zbyněk RAIDA

Dept. of Radio Electronics, Brno University of Technology, Purkyňova 118, 612 00 Brno, Czech Republic

xpokor33@stud.feec.vutbr.cz, xhorak23@stud.feec.vutbr.cz, raida@feec.vutbr.cz

**Abstract.** The paper briefly uncovers techniques used for a design of compact planar antennas in order to achieve the wideband and the multi-band capability. The main topic is aimed to the multi-objective optimization using genetic algorithms.

A quarter-wavelength planar inverted-F antenna (PIFA) using a slot and shorted parasitic patches is chosen to cover GSM900, GSM1800 and ISM2400 bands.

A global multi-objective optimization uses a binary genetic algorithm with a composite objective function to tune this antenna. The impedance match and the direction of maximum gain are desired parameters to improve.

## Keywords

Multi-objective optimization, multi-band antenna, planar antenna, genetic algorithm, GSM, ISM, Matlab, IE3D.

## 1. Introduction

Currently, the wireless and mobile communications are one of the most growing branches. The demand for hand-held devices operating in a wide spectrum of wireless applications involves miniature and multi-band antennas. Only high-quality equipments can be successful at the market [1], [2], [3].

The planar antenna is a conducting patch printed on a grounded microwave substrate. Due to this, the low profile and the low cost manufacturing are achieved [4]. On the other hand, the bandwidth is extremely narrow [1], [2]. In recent years, many techniques, which allow the increase of the bandwidth, have been published; e.g., advanced microwave substrates as the low-permittivity materials (FoamClad [5]) and EGB substrates [6], or the geometric elements as additional parasitic resonators, slot-loading patches and elevated ones [1].

The CAD systems are necessary for the design of planar antennas. In order to achieve usable or excellent performance of the antenna, the optimization process is essential [3], [4]. This paper is concentrated on the multi-objective optimization using genetic algorithms (GA).

## 2. Antenna Description

As mentioned earlier, the PIFA has been chosen for the investigation. It is a typical antenna for mobile devices in commercial applications. The following paragraphs clarify the techniques used, which have been published in [1] and [2].

### 2.1 Size Reduction Techniques

The ordinary patch antenna is operated in  $\lambda/2$  resonance, where  $\lambda$  is the wavelength. It is clear that the insertion of the shorting wall in the middle of the patch has no influence on the electric field distribution (see Fig. 1). Then a one half of the structure can be discarded so a half-dimension patch antenna operating in  $\lambda/4$  resonance can be obtained.

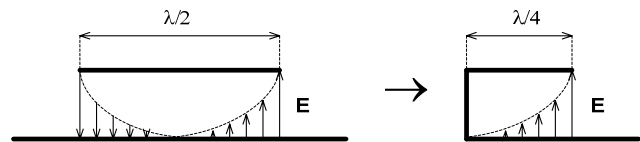


Fig. 1. Converting  $\lambda/2$  structure into  $\lambda/4$  one in order to reduce the antenna size.

Furthermore, the decrease of a resonant frequency is provided by a reduction of a shorting wall almost into a single point. It is due to the elongation of surface currents (see Fig. 2).

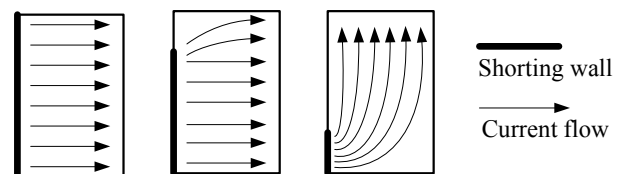


Fig. 2. Influence of the shorting wall on surface currents.

### 2.2 Multi-Band and Broadband Techniques

The narrow bandwidth is typical for planar antennas. The bandwidth is inversely proportional to the quality factor  $Q$  which is defined for a common resonator as:

$$Q = \frac{\text{Energy stored}}{\text{Energy lost}} \quad (1)$$

The low permittivity substrate is used in this design, because it tends to radiate energy more than store it. Further reduction of the energy stored is provided by an elevation of the antenna above the ground plane. That way, the value of the quality factor is decreased, and the bandwidth is increased. Multi-band and broadband capabilities are achieved by:

- Embedding the suitable slot into the main patch in order to create the dual-band antenna;
- Doubling the main patch resonances by using two parasitic gap-coupled resonators,
- Creating a new band by using a single parasitic gap-coupled resonator.

### 2.3 Antenna Design

In the first step, we adopt the antenna construction concept described in [1]. Unfortunately, the antenna can be hardly manufactured (see Fig. 3), because it represents a complex self-supporting construction, and therefore, the patch and its components have to be made only of the metallic plates, which demand an accurate fabrication and assembly of antenna elements. Therefore, we decided to completely redesign the published antenna.

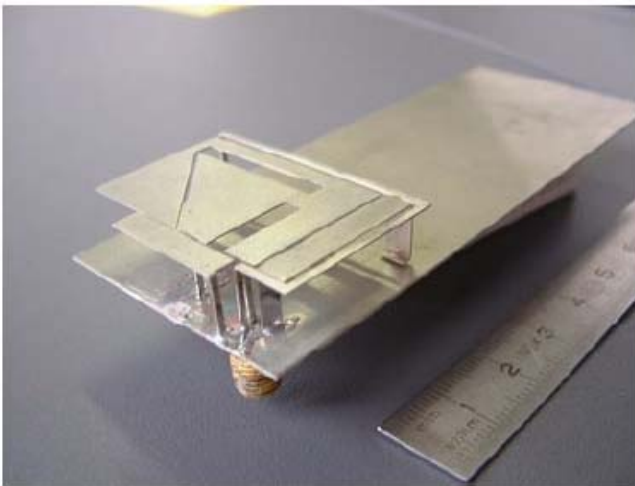


Fig. 3. The original structure of the multiband antenna [1].

The redesign was carried out by applying the above-described techniques and using the IE3D electromagnetic simulator [7]. The feeding is provided by a coaxial probe through the ground plane. Antenna elements are made of the DiClad870 substrate [5], and the ground plane is made of the FR4 substrate. A printed-circuit technology, premised for the antenna manufacture, provides the accurate dimensions and layout of antenna elements. The resultant original antenna structure and its dimensions are shown in Fig. 4.

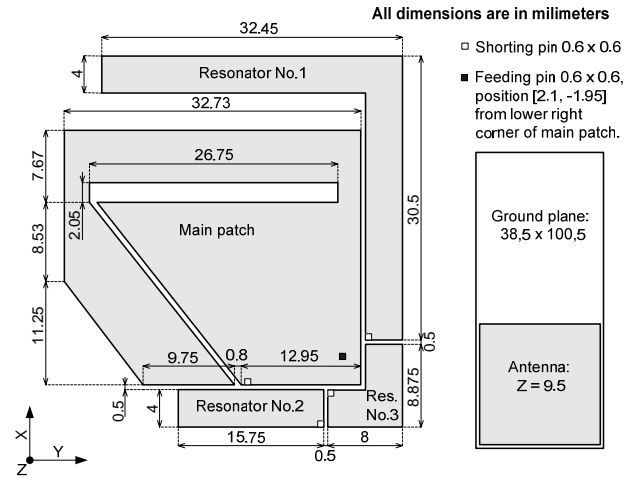


Fig. 4. Dimensions of the designed antenna.

Main patch resonances cover lower halves of the GSM900 band and the GSM1800 ones. The resonator no. 1 covers the upper half of the GSM900 band, the resonator no. 2 covers the upper half of the GSM1800 band, and the resonator no. 3 covers the whole ISM2400 band. The frequency response of the reflection coefficient at the feeding point ( $|S_{11}|$ ) and radiation patterns properties are mentioned later in comparison with the optimized antenna.

### 3. Genetic Algorithm

The binary-coded genetic algorithm (GA) is used to improve the performance of the designed antenna. GA is a population based algorithm using the binary representation of variables (genes) merged into the binary string (chromosome) [3], [4], [8]. The working principle of the used GA is shown in Fig. 5. The whole optimization process is performed by MATLAB except of the antenna analysis (IE3D is used).

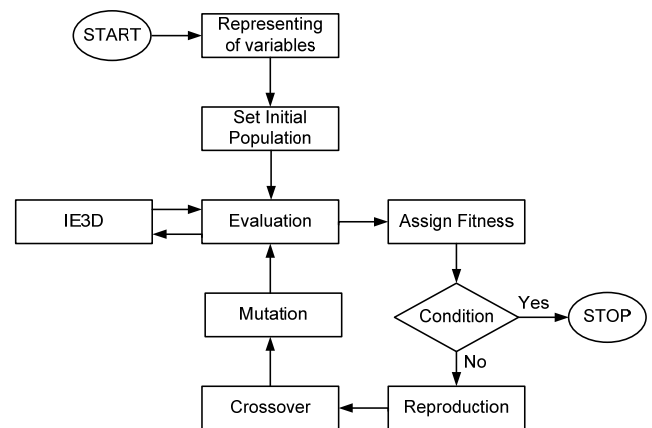


Fig. 5. A flowchart of the working principle of the used GA.

#### 3.1 Representing Variables

The antenna is described by 19 variables, and all of them are used in the optimization process. Only 18 vari-

ables are shown in Fig. 6. The 19<sup>th</sup> variable is the antenna elevation above the ground plane.

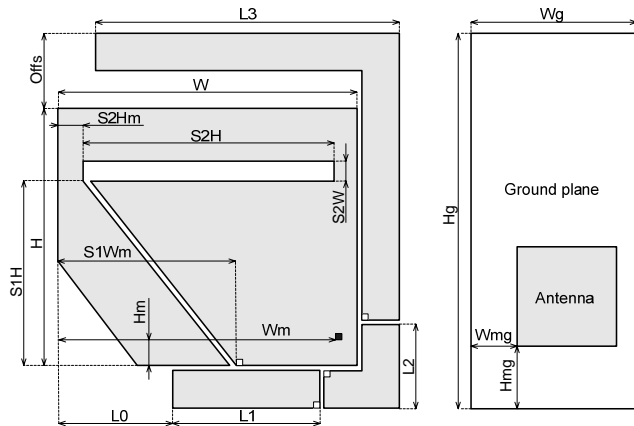


Fig. 6. Set variables for optimization.

It is important that any combination of variables has to represent the feasible individual. Therefore, suitable constraints and relations between variables have to be set. Each variable is coded in the 8 bit resolution, which leads to the 153 bit long chromosome.

### 3.2 Setting Initial Population

If no solution is known, the whole population consists of random individuals [3], [8]. But in our case, the designed antenna was described by the defined discrete variables, so that an initial individual is obtained. Then the initial population consists of:

- Five random individuals;
- Five individuals derived from the initial individual by applying the mutation with the probability of 2%;
- Five individuals derived from the initial individual by applying the mutation with the probability of 20%;
- One individual identical to the initial one.

### 3.3 Evaluating and Assigning Fitness

The chromosome of each individual in the current population is decoded, so that variables values are obtained. Then the coordinates of antenna vertices are computed, and a geometry file for IE3D is created. The antenna performance is evaluated at five frequencies (see Tab. 1.). Four frequencies are identical with the boundary frequencies of GSM900 and GSM1800 bands. The fifth frequency corresponds to the center frequency of the ISM2400 band. IE3D returns values of  $|S_{11}|$  and the radiation patterns properties.

The global multi-objective function that is going to be minimized by the GA consists of the following criteria.

- The impedance match objective function:

$$F_1 = \sqrt{\frac{\sum_i^N (|S_{11}|_i)^2}{N}} \quad (2)$$

where  $N$  is the number of evaluated frequencies and  $|S_{11}|_i$  is the magnitude of the reflection coefficient at the  $i^{\text{th}}$  frequency. The value of  $F_1$  is from the interval  $\langle 0, 1 \rangle$ , where 0 corresponds to a perfect impedance match at all frequencies.

- The maximum gain direction objective function:

$$F_2 = \sqrt{\frac{\sum_i^N (\theta_i / 180)^2}{N}} \quad (3)$$

where  $N$  is the number of evaluated frequencies and  $\theta_i$  is an angle [degree] at the maximum gain measured from the  $Z$  axis at the  $i^{\text{th}}$  frequency. The value of  $F_2$  is from the interval  $\langle 0, 1 \rangle$ , where 0 corresponds to the positive  $Z$  axis direction and 1 corresponds to the negative  $Z$  axis direction of the maximum gain at all frequencies.

Now the double-objective function can be expressed as:

$$F = \sqrt{\frac{(w_1 F_1)^2 + (w_2 F_2)^2}{w_1^2 + w_2^2}} \quad (4)$$

where partial objective functions  $F_1$  and  $F_2$  are weighed by coefficients  $w_1$  and  $w_2$ .

The value of  $F$  is also from the interval  $\langle 0, 1 \rangle$ . When minimizing  $F$ , a better solution can be obtained.

Each individual of the current population is assessed by the computed value of  $F$ , which represents a fitness of an individual. The lower the value of  $F$  is, the better the quality of the individual is.

### 3.4 Reproduction

The primary objective of a reproduction operator is to privilege good individuals and handicap bad ones when creating a population children; the population size has to be kept constant.

There are many ways to achieve the task above. In our case, the tournament selection was implemented as a method of the reproduction. Tournaments are played between two individuals (solutions). The better individual (the solution with the lower value of the fitness) is chosen and placed into the mating pool. Each individual can be made to participate in exactly two tournaments. The best individual will win both times and two copies of it will be placed in the mating pool. The worst individual will lose both tournaments and no copies of it will be created [8].

The initial population (16 individuals) is sorted upwards by the fitness value. The first 12 individuals are

chosen to play the tournament, and thereby create 12 copies in the mating pool.

### 3.5 Crossover and Mutation

In order to create a new generation of individuals, crossover and mutation operators have to be applied. In case of the crossover operator, two individuals are picked from the mating pool at random and some portions of chromosomes are exchanged between the individuals to create two new individuals [3], [8].

The dual-point crossover and six coupled individuals chosen at random from the mating pool are used to create six offspring. The bitwise mutation operator is applied to provide search aspect of GA. The operator inverts a random bit in a chromosome of an individual picked from the mating pool with a probability of 5%. Moreover, if a new offspring is created by the crossover, and its chromosome is already present in the current population, then the mutation operator is automatically applied on it.

That way, new seven individuals are created. The worst seven individuals in the current population are replaced by them, so the new population is set.

## 4. Results

In this section, the results obtained by two approaches – by the single-objective optimization (SOO) using  $F_1$  only to assess individuals, and by the double-objective optimization (DOO) using  $F_1$  and  $F_2$  joined into the global objective function  $F$  for assessing individuals.

### 4.1 Single-Objective Optimization

The progress of the lowest fitness value in the population during 150 iterations is shown in Fig. 7. The convergence of GA is quite fast. After 60 iterations, the major improvement is done. Frequency responses of the reflection coefficient are shown in Fig. 8. The significant improvement of the impedance match is evident at all the desired frequencies. Dimensions of the original antenna and the optimized one are given in Tab. 2.

### 4.2 Double-Objective Optimization

The best results were obtained by using weights  $w_1 = 4$  and  $w_2 = 3$ . The progress of the lowest fitness value in the population during 250 iterations is shown in Fig. 9. The convergence of DOO is certainly slower than the convergence of SOO. At the 35<sup>th</sup> iteration the major modification of the antenna is obtained, if the working frequency of resonators No. 2 and No. 3 is swapped (see Fig. 11.). The result is an improvement of maximum gain direction in accordance with a decrease of  $F_2$  function, especially at the ISM2400 band, which is clear from Fig. 12, where simulated radiation patterns are compared.

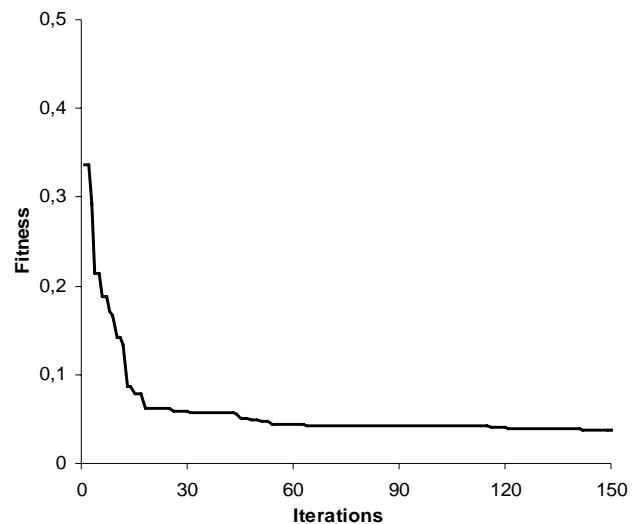


Fig. 7. Progress of the objective function  $F_1$ .

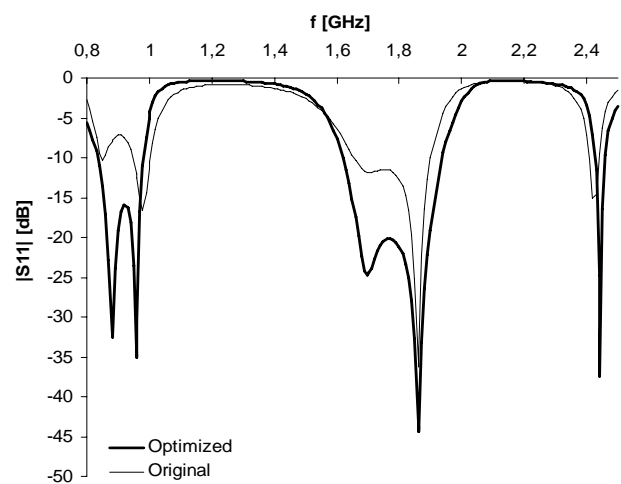


Fig. 8. Frequency response of reflection coefficient of original and single-objective optimized antenna.

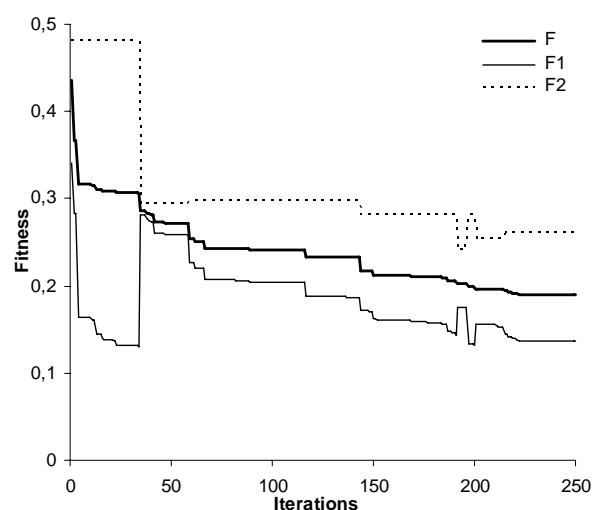


Fig. 9. Progress of objective functions  $F_1$ ,  $F_2$  and  $F$ .

The impedance match at all the desired frequencies is approximately as good as in case of SOO, except of the GSM1800 band. That is clear from the frequency responses of the reflection coefficient in Fig. 10. Dimensions of the original antenna and the optimized one are given in Tab. 2.

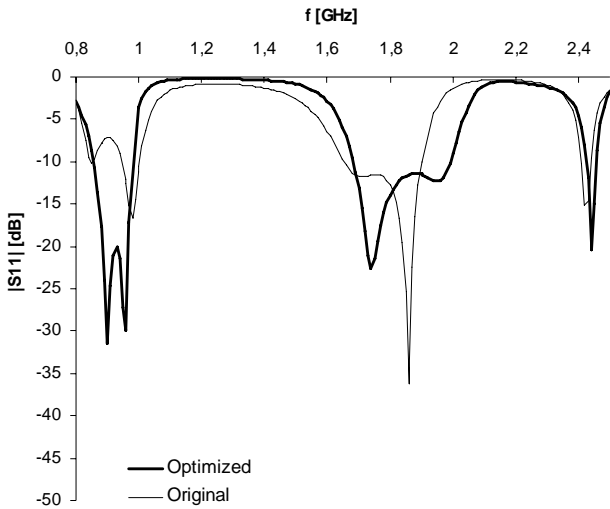


Fig. 10. Frequency response of reflection coefficient of the original antenna and the double-objective optimized one.

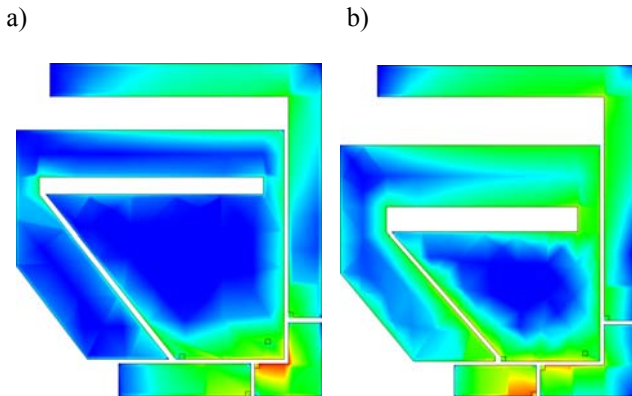


Fig. 11. Current distribution at the center frequency of the ISM2400 band of a) the original antenna, b) the double-objective optimized antenna.

### 4.3 Comparisons

The convergence speed of GA indicated by the number of iterations can be qualified positively. But the time necessary to evaluate all individuals at the single iteration is too high. Finally, the SOO process takes 1 day 3 hours and 16 minutes. The DOO process takes 2 days 12 hours and 21 minutes of the CPU time (AMD Athlon 3000+). The comparisons of the results are presented in Tab. 1. The dimensions of the original antenna and the optimized one are summarized in Tab. 2. Obviously, the significant improvement of the followed objectives was obtained in both cases, but the price is a larger ground plane. It is due to the dependence of the impedance match at the GSM900 band on the ground plane dimensions [1].

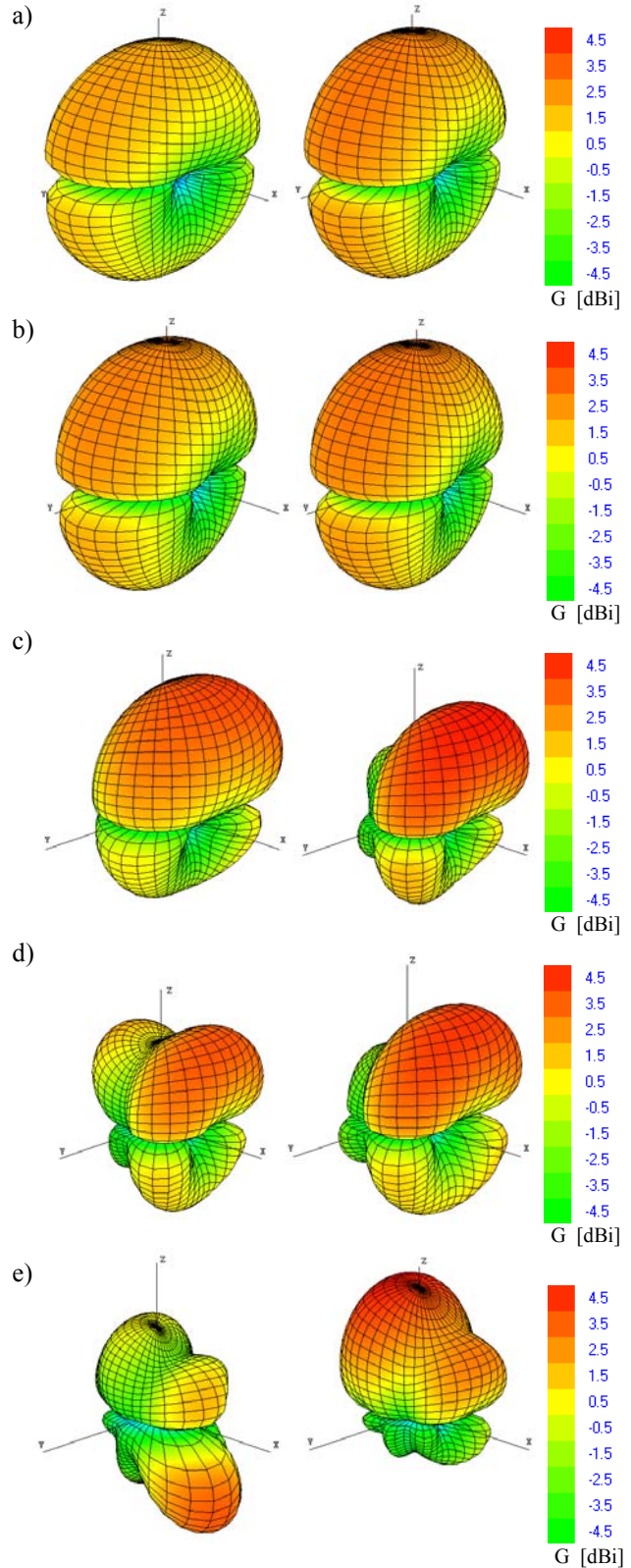


Fig. 12. Total field radiation patterns at a) 0.88 MHz, b) 0.96 MHz, c) 1.71 MHz, d) 1.88 MHz, and e) 2.442 MHz of the original antenna (left) and the double-objective optimized antenna (right). Scales on the right-hand side of patterns define the color representation of gain in dBi.

Frequency [GHz]	Original		Optimized, SOO		Optimized, DOO	
	S <sub>11</sub>   [dB]	θ [°]	S <sub>11</sub>   [dB]	θ [°]	S <sub>11</sub>   [dB]	θ [°]
0.88	-7.8	45	-30.5	45	-24.0	40
0.96	-12.6	35	-27.8	15	-27.2	20
1.71	-11.8	30	-24.3	35	-18.2	35
1.88	-16.5	35	-26.4	40	-11.4	35
2.442	-8.6	120	-34.2	115	-20.4	15

Tab. 1. Comparison of reflection coefficients and θ angles at the maximum gain of the original antenna and the optimized one.

Variable	Original [mm]	Optimized, SOO [mm]	Optimized, DOO [mm]
W	32.73	32.65	32.80
H	27.45	27.10	27.40
S2W	2.05	2.00	1.70
S2H	26.85	26.65	24.15
S1H	19.78	17.90	16.50
S2Hm	3.00	3.01	5.85
S1Wm	18.98	20.35	20.25
Wm	30.48	30.40	30.60
Hm	1.80	1.65	0.70
L0	12.98	12.55	14.40
L1	15.75	15.95	10.35
L2	8.88	8.85	9.15
L3	32.45	31.65	32.60
Offs	8.10	12.95	10.10
Wg	38.50	38.40	44.15
Hg	105.10	129.80	125.10
Wmg	1.00	0.00	6.85
Hmg	1.00	0.90	0.95
Z	9.50	9.50	9.50

Tab. 2. Final variables values of the original antenna and the optimized one.

### 5. Modal Analysis

The modal analysis of the DOO antenna was performed in order to uncover all possible resonances without relation to the feeding. So the coaxial probe was removed from the IE3D model, and the antenna was excited by the perpendicular incident plane wave. Then the current distribution was computed in the frequency range from 0.10 GHz to 3.00 GHz with the step size 0.01 GHz. Each local maximum of the current density across the frequency range at any antenna region was considered as the resonance.

The described method of the modal analysis was used due to the complexity of the antenna geometry: more conclusive approaches using eigenmode solvers are difficult to

perform in such a case. The analysis can reveal resonant frequencies (modes), which are not excited due to feeding implementation.

Tab. 3 shows all the detected resonant frequencies of the antenna excited by the plane wave in comparison with resonant frequencies determined as the local minimum of the coefficient |S<sub>11</sub>| of the antenna fed by the coaxial probe.

Deviations of resonant frequencies no. 1 and 3 of the antenna excited by the plane wave and the antenna fed by the coaxial probe are significant. This is caused by the fact that these resonances correspond to the main patch, which current distribution is significantly affected by the antenna feeding. However, deviations of resonant frequencies no. 2, 4, 5 and 6 are almost negligible because these resonances, which correspond to the current distribution of parasitic gap-coupled resonators, are practically independent on the feeding implementation.

The resonance no. 6 was not included in previous investigations. We discuss this mode here because it was revealed in the selected frequency range of the modal analysis. The resonance no. 6 is very poor, and is provided by the parasitic resonator no. 1.

Resonance number	Plane wave excitation	Coaxial probe feeding
	f [GHz]	f [GHz]
1	0.79	0.90
2	0.96	0.96
3	1.54	1.74
4	2.02	1.95
5	2.39	2.44
6	2.71	2.71

Tab. 3. The set of the detected resonant frequencies of the plane wave excited DOO antenna and the coaxial probe fed DOO antenna.

The current distributions of the DOO antenna at the resonance frequencies are shown in Fig. 13. The distributions of the antenna excited by the plane wave are depicted on the left; the distributions of the antenna fed by the coaxial probe are depicted on the right.

### 6. Realization and Measurement

The original antenna and the DOO one were manufactured. Antenna elements were made of DiClad 870 ( $\epsilon_r = 2.33$ ,  $\tan \delta = 0.0013$ ,  $h = 0.508$  mm) and the ground plane was made of FR4 ( $\epsilon_r = 4.7$ ,  $\tan \delta = 0.03$ ,  $h = 1.5$  mm). The shorting pins and the feeding pin were made of short rectangular profile wires. They are part of “jumper” connectors and their dimensions are 0.6 mm × 0.6 mm × 11 mm. The coaxial probe was provided by the standard 50-ohm connector of the SMA-f type. The photo of the antennas built is given in Fig. 14.

Band	Original	Optimized, DOO
	max $ S_{11} $ [dB]	max $ S_{11} $ [dB]
GSM900	- 9.9	- 12.7
GSM1800	- 10.7	- 12.3
ISM2400	- 5.8	- 5.3

Tab. 4. Maximal values of the measured frequency response of the reflection coefficient of the realized antennas in the range of the desired frequency bands.

The frequency response of the reflection coefficient was measured by the network analyzer AGILENT E8364B. The measured results are shown in Fig. 15. Both antennas provide good performance in full range of the operation frequency bands as shown in Tab. 4. Only the ISM2400 band is slightly out of the working frequency. The deviation is about 40 MHz for the original antenna and -35 MHz for the DOO antenna. The comparison of the computed and measured frequency response of the reflection coefficient is shown in Fig. 16 for the original antenna, and in Fig. 17 for the DOO optimized one. Both characteristics prove a sufficient agreement, but some obvious differences are present. The most significant impedance match disagreements at the lower half of GSM900 band of the original antenna and at the upper half band of GSM1800 of the DOO optimized one and the frequency shift are caused mainly by a manual assembly and soldering of the antenna and the metal pins.

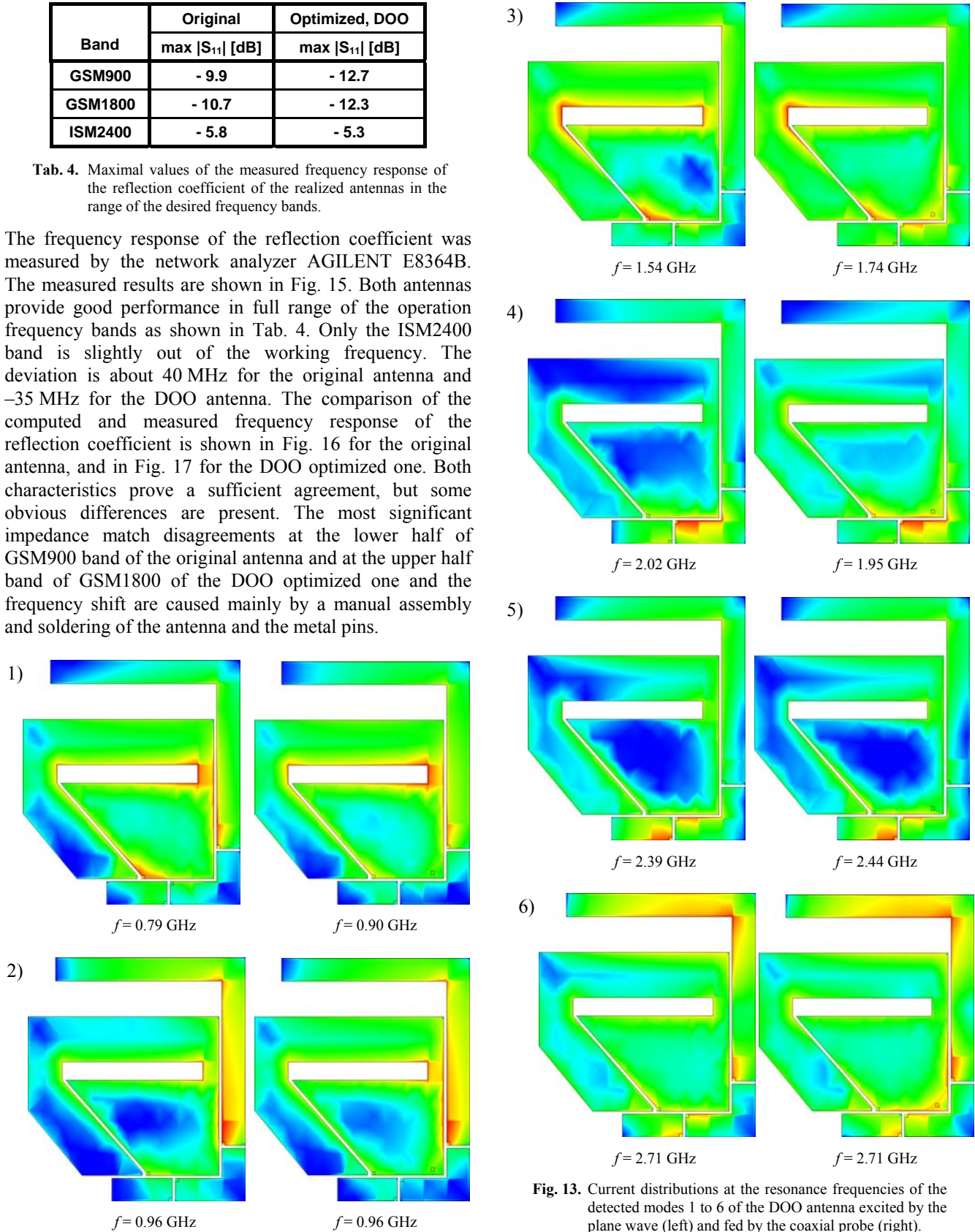


Fig. 13. Current distributions at the resonance frequencies of the detected modes 1 to 6 of the DOO antenna excited by the plane wave (left) and fed by the coaxial probe (right).



Fig. 14. Photographs of the realized antennas: a) the original one, b) the double-objective optimized one.

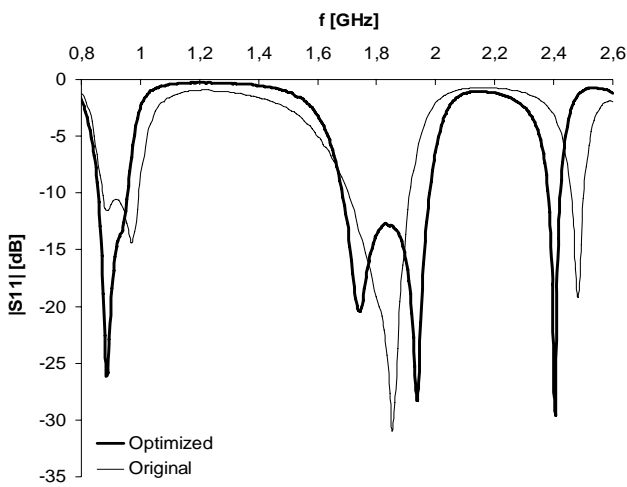


Fig. 15. Measured frequency response of the reflection coefficient of the realized antennas.

Thanks to the cooperation with the Czech radar company ERA Pardubice, measurements of the radiation patterns were performed in the anechoic chamber. The measured results are shown in Fig. 18 where the simulated and measured gain magnitude is presented in the normalized form, because the absolute value of gain is not available. So, only the shape of the simulated and measured patterns can be compared. Due to IE3D computation feature, the calculated patterns have zero fields forced in the horizontal plane.

Both antennas can be approximately classified as omnidirectional ones in the upper-half space only, because there are some strong extremes in the lower half-space.

The antennas provide both linear polarizations in each frequency band with the different gain and radiation pattern. However, no one can be classified as dominant. It is the great advantage for hand held devices where the arbitrary spatial orientation of the antenna is assumed.

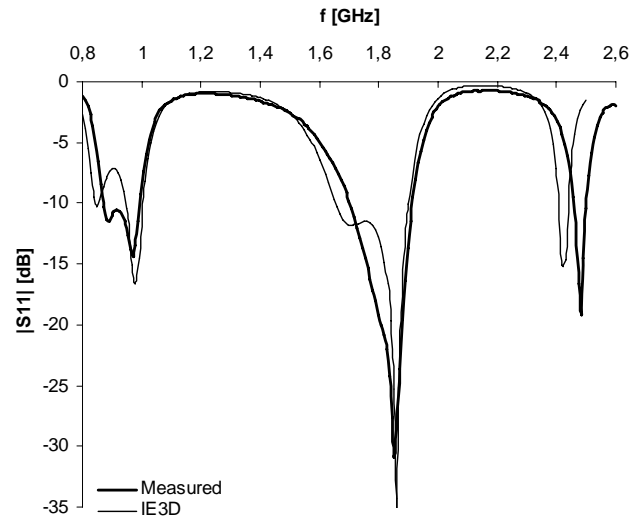


Fig. 16. The measured and simulated frequency response of the reflection coefficient of the original antenna.

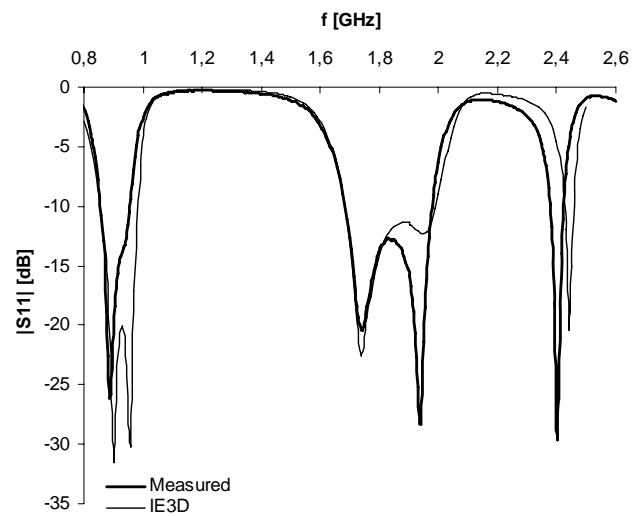


Fig. 17. The measured and simulated frequency response of the reflection coefficient of the DOO antenna.

## 7. Conclusions

The paper presents the design of the compact tri-band antenna suitable for hand-held devices. The multi-objective optimization using genetic algorithms is chosen to provide the improvement of the impedance match and the direction of the maximum gain.

The results of the single-objective and double-objective optimization are compared. In both cases the significant improvement of the impedance match is obtained. In case of the double-objective optimization, the new con-

stellation of antenna elements with better pattern properties is obtained.

The measurements of the realized double-objective optimized antenna proof the very good performance at all the desired frequency bands.

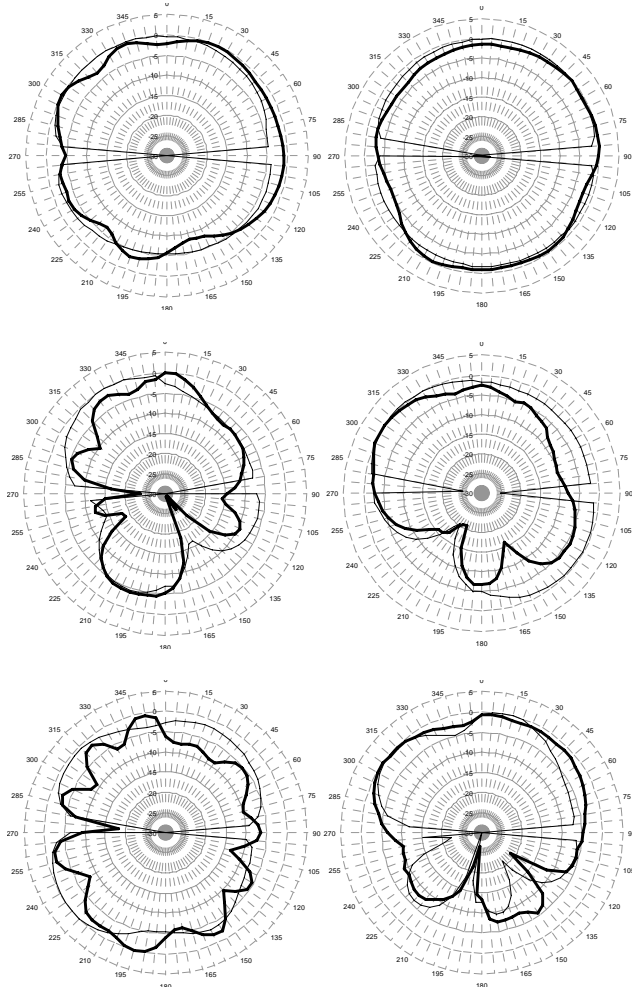


**Fig. 18.** Vertical polarization patterns in YZ plane for 920 MHz (top), 1795 MHz (middle) and 2442 MHz (bottom). The original antenna (left), the double-objective optimized antenna (right). Simulated (thin line), measured (bold line).

## Acknowledgements

The research was supported by the Czech Grant Agency under the grant 102/07/0688, and by the Czech Ministry of Education under the research plan no. MSM 0021630513. The described research is also a part of the COST project IC0603 ASSIST.

## References

[1] CIAIS, P., STARAJ, R., KOSSIAVAS, G., LUXEY, C. Design of an internal quad-band antenna for mobile phones. *IEEE Microwave and Wireless Components Letters*, 2004, Vol. 14, no. 4, p. 148 - 150.

[2] KHOO, C. W. *Multiband Antenna for Handheld Transceivers*. Bachelor thesis. Ipswich: The University of Queensland, Online: <http://innovexpo.itee.uq.edu.au/2002/projects/s4000751/thesis.pdf>.

[3] RAIDA, Z. *Optimization in Electrical Engineering*. Online: <http://www.urel.feec.vutbr.cz/~raida/optimalizace/index.htm>

[4] ČERNOHORSKÝ, D., RAIDA, Z., ŠKVOR, Z., NOVÁČEK, Z. *Analýza a optimalizace mikrovlnných struktur* (Analysis and Optimization of Microwave Structures). Brno: VUTIUM Publishing, 1999. (In Czech.)

[5] *Arlon Product Datasheets*. Rancho Cucamonga: Arlon-MED., 2006.

[6] HERAS, E., RAIDA, Z., LAMADRID, R. Quad-band U-slot antenna for mobile applications. *Radioengineering*, 2006, vol. 15, no. 2, p. 22 to 29.

[7] *IE3D Reference Manual*. Fremont: Zeland Software Inc., 2006.

[8] DEB, K. *Multi-Objective Optimization using Evolutionary Algorithms*. New York: John Wiley & Sons, 2001.

## About Authors...

**Michal POKORNÝ** was born in 1983. He is PhD student at the Brno University of Technology at the Dept. of Radio Electronics. His research interests are antenna design and modeling of microwave semiconductor devices.

**Jiří HORÁK** was born in 1981. He received Ing. (M.Sc.) degrees from the Brno University of Technology (BUT) in 2005. Nowadays he is PhD student at the BUT at the Dept. of Radio Electronics and he is focused on planar antennas with advanced substrates.

**Zbyněk RAIDA** received Ing. (M.Sc.) and Dr. (Ph.D.) degrees from the Brno University of Technology (BUT) in 1991 and 1994, respectively. Since 1993, he has been with the Dept. of Radio Electronics of BUT as the assistant professor (1993 to 1998), associate professor (1999 to 2003), and professor (since 2004). From 1996 to 1997, he spent 6 months at the Laboratoire de Hyperfréquences, Université Catholique de Louvain, Belgium as an independent researcher.

Prof. Raida has authored or coauthored more than 80 papers in scientific journals and conference proceedings. His research has been focused on numerical modeling and optimization of electromagnetic structures, application of neural networks to modeling and design of microwave structures, and on adaptive antennas.

Prof. Raida is a member of the IEEE Microwave Theory and Techniques Society. From 2001 to 2003, he chaired the MTT/AP/ED joint section of the Czech-Slovak chapter of IEEE. In 2003, he became the Senior Member of IEEE. Since 2001, Prof. Raida has been editor-in-chief of the *Radioengineering* journal (publication of Czech and Slovak Technical Universities and URSI committees).